Identification of Incipient Slip Phenomena Based on The Circuit Output Signals of PVDF Film Strips Embedded in Artificial Finger Ridges

Yoji Yamada[1], Takashi Maeno[2], Isao Fujimoto[1], Tetsuya Morizono[1] and Yoji Umetani[1]

1 Toyota Technological Institute 2-12-1, Hisakata, Tenpaku, Nagoya 468-8511, Japan
2 Keio University 3-14-1, Hiyoshi, Kohoku-ku, Yokohama 223-8522, Japan
yamada@toyota-ti.ac.jp, maeno@mech.keio.ac.jp, s2sfuji@toyota-ti.ac.jp

Abstract: This paper deals with development of compliant artificial finger skin surface ridges with a pair of PVDF film strips embedded in each of them as sensing transducers for incipient slip detection in pursuit of elucidating the mechanism of human static friction sensing. We describe design and manufacture of the surface ridges and distinctive detection of incipient slip from rolling.

Keywords: tactile sensor, incipient slip, PVDF, stress rate, roll

1. Introduction

Most of the conventional approaches to construction of various robot tactile sensor mechanisms hold a fundamental problem of a spatial limitation when they are attempted to be mounted on a small area of a robot fingertip for integration of their individual functions. This is because the limited space at a robot fingertip cannot house many sensor mechanisms without causing any mechanical interference with one another. By contact, a variety of human tactile perceptions are attained through integrated processing of tactile information from only several kinds of mechanoreceptors. Therefore, we consider it very important to build a tactile sensing system based upon a design policy of taking the behavior of tactile sensing elements and the tissue embedding them at the same time. Consequently, it becomes worth notice to realize artificial finger skin with sensing elements incorporated into the skin tissue so that they can be expected to have various robot tactile perception capabilities under a novel platform concept: the sensing elements should have a wider frequency detectable range and acquire meaningful information by their elaborate spatial allocation. In the study, we demonstrate the effectiveness of this design policy by pursuing incipient slip detection which plays an important role in elucidating the static friction sensation mechanism.

For this purpose, we decided to attain vibrotactile sensing capabilities on a skin tissue that has softness like humans. Early, Johansson et al.[1)] examined in their study of human static friction sensation that a parallel change in the grip and the load forces is observed during precision grip of an object and the ratio between the two forces is adapted to result in the static friction coefficient between the finger skin surface and the object. According to their suggestion that insipient slip information should play an important role in such precision grip, several studies on robotic incipient slip detection have been reported. Gaetano et al. [2)] proposed a tactile sensor system capable of detecting the incipiency of slip between an object and the sensor surface using the normal and shear stress information from arrays of PVDF transducers. They showed by both simulation and experimentation that a trained neural network with the normal and shea stress signal patterns allowed them to find the incipient slip. However, this method is different from the standard detecting method of incipient slip: An object in contact with a rubber surface is slid on a curved surface and the peripheral area of the contact is initiated to slip.

In this respect, Tremblay et al. [3)] demonstrated the effectiveness of incipient slip detection more early using the peripheral slip signal from accelerometers which were mounted on a curved soft surface.

Similarly, J. S. Son et al.[4)] also devised the surface of the rubber skin to have molded surface texture with arrayed tiny nibs for the purpose of easily obtaining the incipient slip. However, we can still design better shape and structure of the skin surface ridges with vibrotactile sensing elements because the mechanical behavior of nibs and the directivity of the sensors are not necessarily optimized in the above two proposals due to their separate allocation. As the background of establishing a novel design strategy, we have studied the dynamic response of human finger skin for tactile receptors focusing on the effect of epidermal ridges using FE analysis [5)]. We have also proposed to detect impulsive high-frequency vibratory signal at robotic finger surface ridges where PVDF film strips are embedded for isolating a slip phase from various other contact phases [6)].

Moreover, what kind of transducers with 20 dB/dec or higher order dynamic sensing characteristics we should use is also an important technical issue. Though the above approach by Tremblay et al. to using accelerometers is considered to have higher sensitivity in acquiring vibrotactile information, they cannot be easily downsized. PVDF film transducers which were introduced to this study field by Dario et al. [7)] are promising due to their flexibility and high sensitivity. Later work on texture distinguishment by Patterson et al. [8)] is also notable, from the viewpoint that the work was the first proposal of using the PVDF film transducers in dynamic tactile sensing which is a widely applicable concept developed by Howe et al.[9)] They also used the same PVDF film transducers referring to it as stress rate sensor in their work on monitoring contact conditions for dextrous robot hand manipulation. It is interesting to note that a PVDF transducer has the possibility of exhibiting various frequency characteristics in connection with an amplifier [10)]

In this study, we show the development process of artificial finger skin surface ridges in each of which a pair of PVDF film strips are embedded. The design process of the artificial finger skin regarding the shape and size is described in chapter 2. In chapter 3, the frequency characteristic of a PVDF circuit is examined with the equivalent circuit modeled. We demonstrate in chapter 4 that the sensing function of the artificial finger skin allows us to detect the incipient slip and use a minimum phase FIR digital filter to remove a high-frequency signal. When a robot hand manipulates an object, slipping and/or rolling contact can be observed, and two contact phases must be distinguished from each other. Whether they can be distinguished or not is examined in chapter 5. The conclusion for this study is finally made in chapter 6.

2. Design Processes of Artificial Skin

2.1 Design Processes of Artificial Skin

In this study, there are two processes of designing artificial finger skin which are schematically described in **Figure 1**. The first proce-

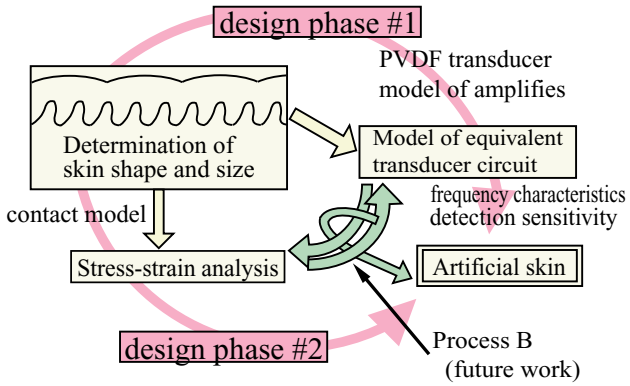

Figure 1: Design process of artificial finger skin

ss A consists of two design phases; design ♯1 and ♯2. Design phase ♯1 is to examine the frequency characteristics and the sensitivity of the transducer circuit used in the artificial finger skin. We select PVDF film as the transducer of artificial mechanoreceptors because the film has high mechanical flexibility and we can expect high sensitivity of piezoelectricity with dynamic responses of technical interest. We consider that this phase of determining the equivalent circuit of the PVDF film in connection with an amplifier is important for later use of designing more desired PVDF transducer circuit. In design phase ♯2, we design the shape and size of the artificial finger skin. In this phase, it is important to identify where the PVDF transducers should be localized and what kind of tactile information from the transducers is significant in detecting the incipient slip. The above two design phases are conducted independently, and reconsidered after taking the other phase into account as the second process to find the optimal design solution to the artificial finger skin with more highly sensitive and reliable incipient slip detection capability.

2.2 Design of the artificial finger skin

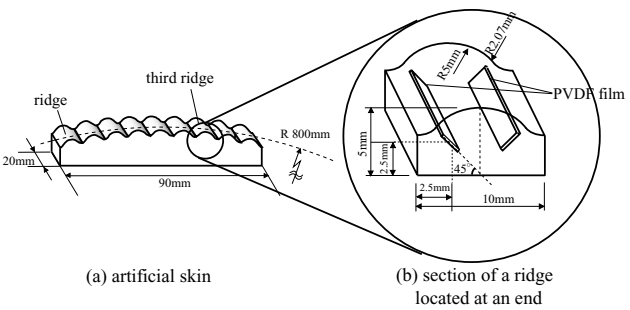

Figure 2: Design of artificial finger skin

In the design phase ♯2, we manufactured an artificial finger skin whose shape and size are designed as shown in **Figure 2**[11]. **Figure 2(a)** shows the artificial finger skin with nine ridges. The detail of one ridge is shown in **Figure 2(b)**. We designed the artificial finger skin imitating the following characteristics of human fingers. First, tissue of a human finger except for bones consists of flexible materials. The materials transform contact information to tactile receptors through elastic deformation of the tissue. Second, a human finger has a curved surface in broad perspective. Third, epidermal ridges are distributed at a finger surface. A pair of FAI receptors is observed to be located at the top dermis papilla underneath one epidermal ridge[12]. It is analyzed by FEM that all of the nine ridges contact a flat object when normal force of 4 N is applied.

3. Examination of the frequency characteristic of a PVDF circuit

3.1 A circuit model and an experimental setup

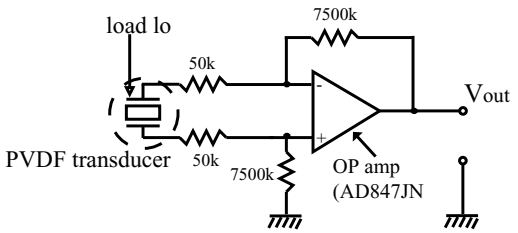

Figure 3: Circuit diagram of a PVDF circuit (a PVDF transducer + a differential amplifier)

Figure 3 is the circuit diagram of a PVDF circuit composed of a PVDF film transducer followed by a differential amplifier that we produced for our study. The differential amplifier, which is mainly a high input impedance operational amplifier OP amp and plays an important role of rejecting common mode noise, is connected to a PVDF film transducer.

A load *lo* is applied to the PVDF film transducer. It generates electric charges which are converted to output voltage v_{out} by the succeeding differential amplifier. We can monitor the two parameters *lo* and v_{out}, and compute the *Gain* of the linear PVDF circuit system which is defined as

$$Gain = 20log|\frac{v_{out}}{lo}| \quad (1)$$

where *Gain* is a function of frequency $f_{PV} = \frac{\omega}{2\pi}$ because the PVDF circuit exhibits a dynamic characteristic due to the parallelly connected CR circuit components of both the PVDF film and the OP amp input.

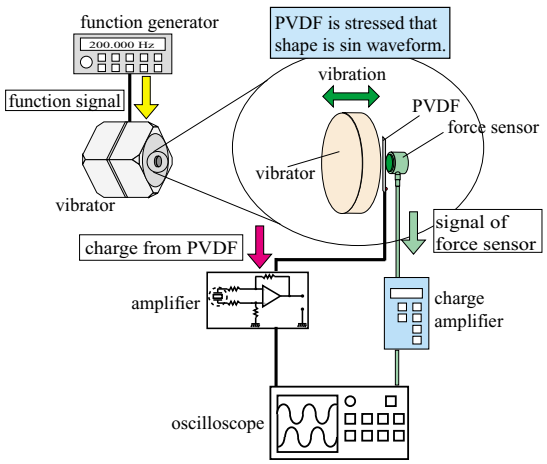

Figure 4: Experimental setup for examining the frequency characteristic of a PVDF circuit

The experimental setup for examining the frequency characteristic of a PVDF circuit is shown in **Figure 4**. The PVDF film transducer is preloaded at 25 N between the indentor of a vibrator and a force sensor probe. The area of the contact plane between the film surface and the indentor is about 8 mm^2. The vibrator is driven by a sinusoidal input signal. The magnitude of the sinusoidal load *lo* is observed by a force sensor, and is kept constant regardless of the input frequency f_{PV} which ranges from 2 to 20000 Hz.

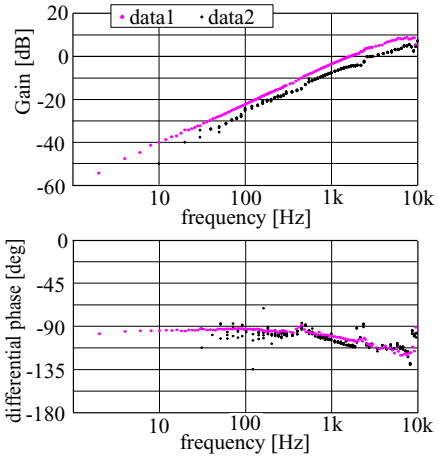

Figure 5: Experimental result

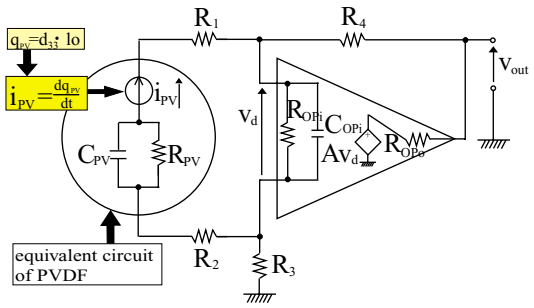

Figure 6: Overall equivalent circuit of the PVDF circuit

3.2 Experimental results

The experimental results of the frequency characteristics of a PVDF circuit are shown in **Figure 5**.

The result of data1 indicates the following points to note. (i) First order (20 dB/dec) frequency characteristic appears in the range from 2 to 2000 Hz. This characteristic is called stress rate which was originally pointed out by Howe et.al.[9]. From the result, we can model the approximated Gain as

$$Gain = 20log_{10}(f_{PV}) + b \tag{2}$$

where b is the value of $Gain$ at 1 Hz. (ii) Gain saturates and the first order frequency characteristic disappears over 2000 Hz. (iii) We can observe rapid drops at f_{PV}=500, 2400, and 9000 Hz. We have already traced that the drops resulted from mechanical resonance of the system comprising the vibrator indentor and the PVDF film.

We also note the following points concerning the result of data2 where 5 kinds of load ranging from 0.2 to 10 N for every sampled frequency are applied to the PVDF film (i) Gain has a linear relation for the load applied. (ii) Comparing data2 with data1, Gain differs when the PVDF film sheet is replaced. If one wants to detect the amount of load applied, the value of b in equation of (2) must be determined.

Our previous report [13] described that this PVDF circuit has stress-rate and stress-jerk characteristics connected in series with a break point at 1.2 kHz. After intensive examination for the characteristics, we hereafter declare that the characteristics need to be corrected almost equivalently as the well-known first-order one as shown in **Figure 5** of this paper.

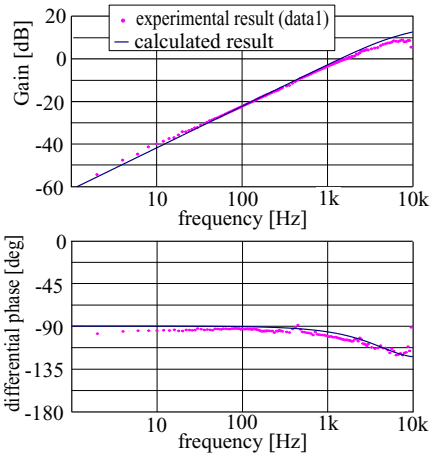

Figure 7: Computed result of Gain(24 dB is subtracted to the calculated result in order to match the experimental characteristic.)

Table 1: Calculated parameter

C_{PV}	3.0×10^{-11} [F]	C_{OPi}	1.5×10^{-12} [F]
R_{PV}	8.0×10^{5} [Ω]	R_{OPi}	3.0×10^{5} [Ω]
		R_{OPo}	15 [Ω]

3.3 A PVDF circuit model

In order to analyze the actual frequency characteristic in **Figure 5**, we propose to apply a parallel CR circuit model to the PVDF transducer as an equivalent circuit. **Figure 6** shows the overall equivalent circuit diagram including that of the succeeding OP amp[14].

Electric charges q_{PV} induced at the electrodes of the polarized PVDF transducer due to the applied stress results from free electrons existing in the vicinity of the electrodes. q_{PV} is proportional to the applied stress lo,

$$q_{PV} = d_{33} lo \tag{3}$$

where d_{33} is the piezoelectric strain constant: d_{33} means the ratio of the charges generated in the 3-axis (in the direction of film thickness) when a mechanical stress is applied to the same 3-axis.

Solving the linear simultaneous equations for the circuit system in **Figure 6**[13], the PVDF circuit gain is formulated as

$$Gain = 20log|(R_{OPo} + A_4)\frac{d_{33} j\omega e^{j\omega t}}{A_3 A_2}| \tag{4}$$

where A_2 through A_4 in formula (4) are developed as follows.

$$A_2 = \frac{R_{OPi}}{R_{OPi} + R_1 + R_2 + R_{PV}(1 - A_1)} \tag{5}$$

$$A_3 = \frac{1}{j\omega C_{OPi} R_{OPi}(1 - A_2) + 1} \tag{6}$$

$$A_4 = \frac{j\omega C_{OPi}}{1 - A_3 + j\omega C_{OPi}(R_3 + R_4 + R_{OPo})} \tag{7}$$

where A_1 is:

$$A_1 = \frac{j\omega C_{PV} R_{PV}}{1 + j\omega C_{PV} R_{PV}} \tag{8}$$

Finally, Gain obtained from (4) through (8) is plotted as the dotted line in **Figure 7** by a use of the parameters in **Table 1**. For comparison, the experimental result of $Gain$ which has been already shown in **Figure 5** is again plotted in the same **Figure 7**. From the two characteristic curves, we conclude that the PVDF circuit can be modeled as shown in **Figure 6** and the circuit gain has a stress rate characteristic.

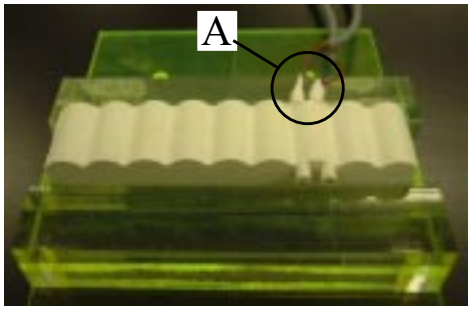

Figure 8: Picture of the manufactured artificial finger skin

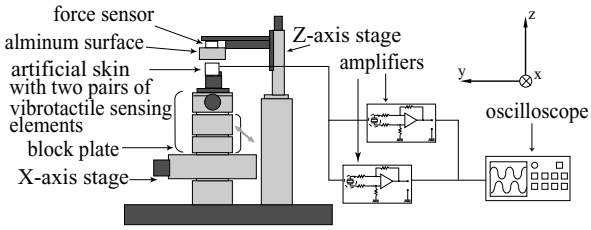

Figure 9: Experimental setup

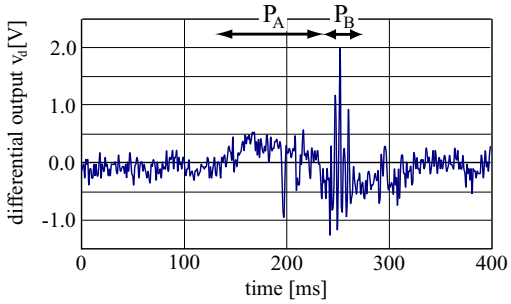

Figure 10: Experimental result

4. Detection of incipient slip

4.1 Experimental setup for generating incipient slip

Figure 8 is a photograph of the manufactured artificial finger skin of 20 mm width, which consists of silicone rubber (KE12:Shinetsu silicone). There are two PVDF film strips of 30 mm length in the third ridge. The glued parts are circled A as shown in the figure. A PVDF film strip is longer than the width of the skin because the glued connection parts between the PVDF strip electrodes and signal wires are harder than the silicone rubber material. If the harder part was in the artificial finger skin, mechanical behavior in the artificial finger skin would be changed. The artificial finger skin was fixed to a thick acrylic substrate.

The experimental setup is shown in **Figure 9**. As shown in the figure, artificial finger skin is fixed to a block plate which is driven in the x and z directions by a x-z stage. The skin is sensitive to slip incipiency in the x direction. The aluminum plate which is in contact with the skin surface at a constant normal force is slid in the x direction. Two channels of the output voltage signals from the third element are monitored at 1000 Hz sampling rate.

The differential signal v_d which was obtained by subtracting two output signals from each other out of a pair of PVDF circuits is depicted in **Figure 10**. In phase P_A of the figure, low-frequency differential signal pattern is observed which contains a small drop component at about 195 steps. The drop of the signal is considered to be resulted from an incipient slip which occurred in the ridge located next to the third according to own simulation results. Phase

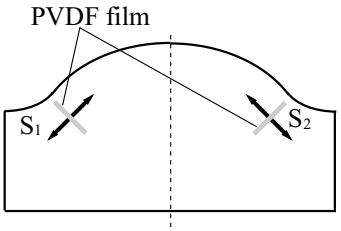

Figure 11: Points and directions for substracting the stress

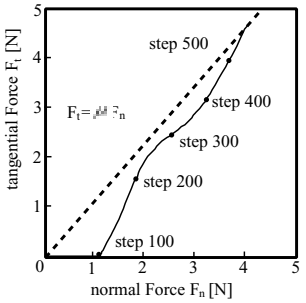

Figure 12: History of external force

P_B is a period in which incipient slip occurred in the ridge. The artificial skin can grasp the slip phenomenon even though a low-frequency signal pattern in the time series of the signal before the incipient slip and the impulsive signal pattern telling the incipiency of the slip are superposed.

Next we show the results of simulation experiments using FEM where incipient slip occurs on the artificial finger skin.

4.2 Simulation of detecting incipient slip

When an external force consisting of a normal and tangential force components, F_n and F_t respectively, is applied to the artificial skin as designed in **Figure 2**, the differential stress signal which is computed from the stresses at S_1 and S_2 in **Figure 11** is analyzed using FEM. The external force is applied as shown in **Figure 12**.

Only a normal force is applied at first. Then, an additional force is applied in the tangential direction of the contact surface. Partial incipient slip nearly occurs from time step 200 to 300, because the divided value F_t/F_n is close to the static friction coefficient. On the other hand, the partial incipient slip does not easily occur from step 300 because the divided value F_t/F_n is considerably smaller than the static friction coefficient. Finally, the partial incipient slip easily occurs again from time step 450 toward the gross slip. All the time is divided into 550 steps. Time of one step is 1.0×10^{-6} s. The computed stress rate component in the third ridge from an end are shown in **Figure 13**. The change of the differential stress is described when incipient slip occurs in the third ridge: First, the differential stress rate increases gradually after the lifting force sta-

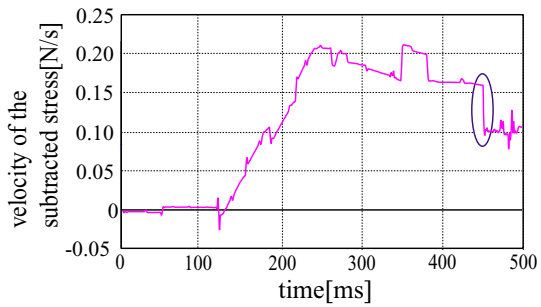

Figure 13: Velocity of the substracted stress inside third ridge

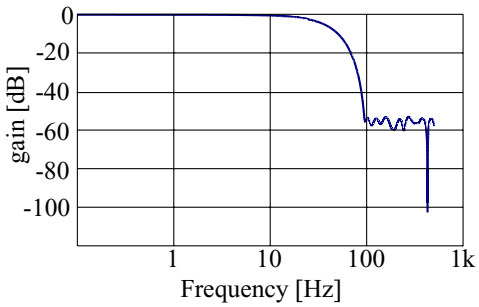

Figure 14: frequency characteristics of FIR fliter

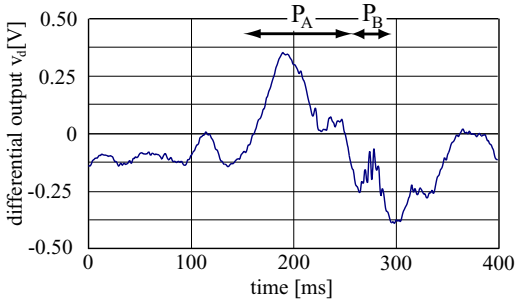

Figure 15: incipient slip signal (after filtered)

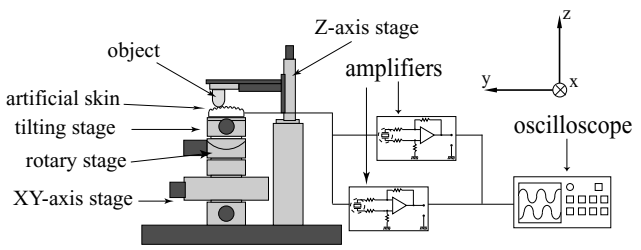

Figure 16: experimental setup

rts to be added. Second, when gross slip occurs in the third ridge, the differential stress rate signal suddenly decreases at step 450 in **Figure 13**.

4.3 Derivation of a low-frequency signal pattern using a FIR digital filter

The signal pattern just before the incipient slip occurs is characterized as a whole by a low-frequency signal component with a high-frequency component of noise superposed. So a signal processor has a potential of misjudgment when the incipient slip occurs. In order to avoid this problem, we designed a minimum phase low pass FIR digital filter for removing the high-frequency noises. The reason why such a FIR filter was used is because a robot hand is required to be controlled as quickly as possible to avoid dropping an object. Thus, a minimum phase filter is used whose phase lag is smallest.

The frequency characteristics (gain) of a minimum phase low pass FIR filter that we designed is shown in **Figure 14**.

The filter in this figure presents a low pass filtering characteristic whose lag phase is 9 degree at 1 Hz and cut off frequency 28 Hz. The result of the data after the above low pass FIR filter is applied is shown in **Figure 15**.

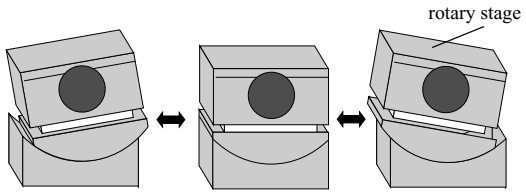

Figure 17: Movement of the rotary stage

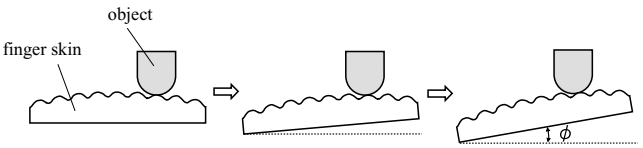

Figure 18: Illustration of a rolling contact between the finger skin and an object

The result shows that a low-frequency signal pattern can be extracted from the original time series signal even when an event of incipient slip occurs and a high-frequency signal component is superposed.

Identification of the incipient slip can be realized as follows. First, a low-frequency signal pattern (**Figure 15**) is extracted for prediction of an incipient slip signal pattern which may succeedingly occur. If such a predictive signal is monitored, a high-frequency signal pattern in the original data during P_B in **Figure 10** exceeds the threshold and the excess will be detected. Finally, if it is detected, this means that an incipient slip phenomenon occurs, and the grasping force of the robot hand can be increased to avoid dropping the object in contact.

5. Distinction of incipient slip from rolling

We showed that we could monitor the patterns of both slip predictive and slip occurring signals, when incipient slip occurred on the artificial finger skin. But we may not be able to isolate incipient slip occurrence because it is anticipated that other types of contact of an object with the skin surface may generate such a high-frequency signal component as shown in **Figure 10**. We set rolling contacts as another typical contact phenomenon when a robot hand manipulates an object. If distinction of incipient slip from rolling is successful, the robot hand does not need useless control action.

The experimental setup for examining the distinction is shown in **Figure 16**. A rolling contact is produced by a use of a moving rotary stage. The movements of the rotary stage are shown in **Figure 17**. The geometric relationship between the artificial finger skin and an object with a semi-spheric head is shown in **Figure 18**. The rotated angle ϕ is 3.5 deg.

The experimental result is shown in **Figure 19**. The two sequences of noisy signals in the figure correspond to the output voltage signals from the pair of PVDF circuits in the third ridge of the artificial finger skin. Bold arrows in the figure point out when a rolling contact occurs. As the results of the experiment, we could observe two patterns of experimental results: one pattern reveals that the two output voltages increased at the same time when a rolling contact was produced as shown in **Figure 19(a)**. In the other pattern, one output voltage sequence generates a positive peak while the other generatesa negative one as shown in **Figure 19(b)**. The filtered result of **Figure 19** is shown in **Figure 20**. Despite

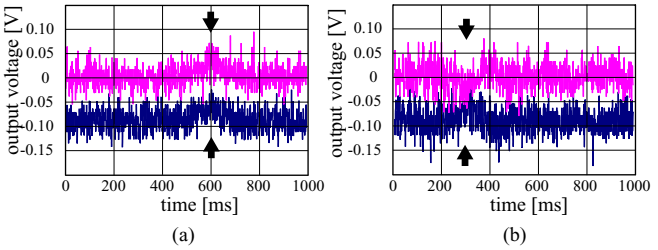

Figure 19: Experimental result of v_d for rolling contact of an object

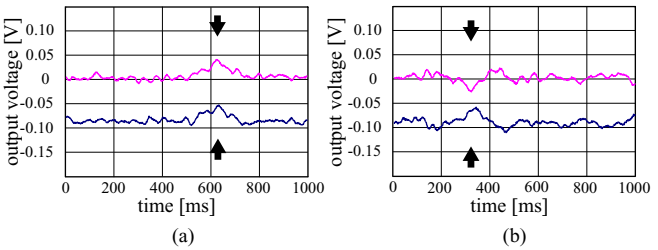

Figure 20: Experimental result of v_d for rolling contact of an object (after filtered)

that there are two experimental result patterns during a rolling contact, both time series signal data do not include any high-frequency component while the signal contains a high-frequency component when an event of incipient slip occurs.

Consequently, We demonstrated distinctive detection of incipient slip from rolling contact by implementation of detecting the combined low- and high-frequency components of the signals. Thus, at first, a low-frequency signal component needs to be extracted for prediction of an incipient slip signal pattern which may include a slip predictive signal as well as a rolling occurrence signal. Next, even when an original series of signal are monitored, however, the signal does not exceed a certain threshold when any rolling contact occurs.

6. Conclusion

In the paper, we described development of artificial skin with vibrotactile sensing elements based upon our design policy for verifying that incipient slip detection plays a central role for static friction sensing. The study is summerized in the following four items.

1. We showed design processes of artificial skin, which was followed by detailed design phases for attaining incipient slip detection.
2. We designed PVDF circuits and examined the frequency characteristics. We showed that the PVDF circuit displayed a stress rate characteristic, and modeled the equivalent circuit consisting of a parallely connected a resistance and a capacitance.
3. PVDF film strips were embedded in the artificial finger skin and incipient slip was produced at the contact area with an object. We showed that such an incipient slip could be detected as follows; First, a low-frequency signal pattern was extracted for prediction of a incipient slip signal which might succeedingly occur. If such a predictive signal was monitored, we could attain successful detection of incipient slip. Finally, if the slip occurrence signal was detected, the grasping force of a robot hand could be increased to avoid dropping an object.
4. We manufactured the experimental setup to produce rolling contact phenomena and observed the output from PVDF circuits. The result showed that the time series of signal did not contain any high-frequency component, and we could demonstrate clear distinction of the signal when either incipient slip or rolling occurred through observing the succeeding low- and high-frequency components in the time series of signals.

Acknowledgments

This study was supported by the Ministry of Education, Culture, Sports, Science and Technology under Grant-in-Aid for Scientific Reseach No.10450161.

References

[1] R.S.Johansson et.al.: Tactile sensory cording in the glabrous skin of the human hand, *Trends in NeuroSciences* ,Vol.6, No.1, pp27–32, 1983.

[2] G. Canepa et.al.: Detection of Incipient Object Slippage by Skin-Like Sensing and Neural Network Processing, *IEEE Transactions on Systems, Man, and Cybernetics-Part B: Cybernetics*, Vol.28, No.3, pp.348–356, 1998.

[3] Marc R. Trembly et.al.: Estimating friction using incipient slip sensing during a manipulation task, *IEEE International conference on robotics and automation*, pp.429–434, 1993.

[4] J. S. Son et al.: A Tactile Sensor for Localizing Transient Events in Manipulation, *Proceedings of 1994 Int. Conf. on Robotics and Automation*, pp.471–476, 1994.

[5] T. Maeno et al.: FE Analysis of the Dynamic Characteristics of the Human Finger Pad in Contact with Objects with/without Surface Roughness, *Proc. 1998 ASME International Mechanical Engineering Congress and Exposition*, DSC-Vol.64, pp.279–286, 1998.

[6] Y.Yamada et.al.: Slip phase isolating : impulsive signal generating vibrotactile sensor and its application to real-time object regrip control, *Robotica*, Vol.18, pp.43–49, 2000.

[7] P.Dario et.al.: Piezoelectric Polymers: New Sensor Materials for Robotic Applications, *13th International Symposium on Industrial Robots and Robots 7*, Vol.2, pp.14-34–14-49, 1983.

[8] R.W. Patterson et.al.: The induced vibration touch sensor – a new dynamic touch sensing concept , *Robotica*, Vol.4, pp.27–31, 1986.

[9] R.D.Howe et.al.: Dynamic tactile sensing: Perception of fine surface features with stress rate sensing, *IEEE transactions on robotics and automation*, Vol.9, No.2, pp.140–151, 1993.

[10] Y. Yamada et al.: Primary Development of Viscoelastic Robot Skin with Vibrotactile Sensation of Pacinian/ Non-Pachinian Channels, *Proceeding of the 3rd International Conference on Advanced Mechatronics*, pp.879–885, 1998.

[11] D.Yamada et.al.: Artificial Finger Skin having Ridges and Distributed Tactile Sensors used for Grasp Force Control, *Journal of Robotics and Mechatronics*, Vol.14, No.2, 2002.

[12] Delcomyn. Fred: *Foundation of Neurobiology. '97*, *W.H.Freeman*, 1997

[13] Y.Yamada et.al.: Development of Artificial Skin Surface Ridges with Vibrotactile Sensing Elements for Incipient Slip Detection, *International Conference Multisensor Fusion and Integration for Intelligent Systems*, pp.251-257, 2001.

[14] Sergio Franco: *Design with Operational Amplifiers and Analog Integrated Circuits*, pp.28–33, *McGraw-Hill Book Company*, 1988